International Journal of Advanced Engineering Research and Science (IJAERS)
Peer-Reviewed Journal
ISSN: 2349-6495(P) | 2456-1908(O)
Vol-8, Issue-10; Oct, 2021
Journal Home Page Available: https://ijaers.com/
Article DOI: https://dx.doi.org/10.22161/ijaers.89.31

Peaks and Valleys Model for Risks Mitigation in Financial System: A Method Based in Multilevel Thresholding with OBIA for Change Detections in Agricultural Areas, using Remote Sensing

Sumaia Resegue Aboud Neta[1], Edilson de Souza Bias[1], Rodrigo Nogueira Vasconcelos[2], Osmar Abílio Carvalho Junior[3], Celso Aparecido Martins dos Santos[1]

[1]Institute of Geosciences, National University of Brasilia, Brasília, DF, Brazil.
[2]Department of Earth Sciences and Environmental Modelling, State University of Feira de Santana, Bahia, BA, Brazil.
[3]Institute of Human Sciences, Department of Geography, National University of Brasília, Brasília, DF, Brazil.

Received: 13 Aug 2021,
Received in revised form: 14 Sep 2021,
Accepted: 29 Sep 2021,
Available online: 11 Oct 2021

***Keywords*— Change Detections, Descriptors, LimiariZC, Mitigation, Multilevel Thresholding, Nanosatellites, OBIA, Peaks and Valleys, Python, Remote Sensing.**

***Abstract*—** *The Geotechnologies has contributed to continuous and agile monitoring, allowing strategic decision, such as monitoring by Remote Sensing in the use and land cover with the agribusiness, which is one of the main sectors of the world economy. Agriculture is one of the responsible for the positive balance of trade in several countries and which many have government policies that subsidize agricultural credits to encourage the sector. Thus, it's necessary to mitigate risks in the financeable agricultural areas, with quick and transparent inspection. In this scenario, a tool in Python language was develop containing a method, called of Peaks and Valleys (PV) Model, for remote monitoring of agricultural production with multitemporal changes detections. The study was in an area in Brazil, using 9 images from the Nanosatellite Planet, from 2017 to 2019. The method has a decision tree that was able to detect changes in the patterns of agricultural areas, issuing assertive signals in cases of deviation in behavior in the remote monitoring of cultivation, from initial cycle, full and final of maturation agricultural, with messages of warning of vegetation growth or alert of loss of vegetation. In model a multilevel thresholding is performed and descriptors extracted (Entropy, Homogeneity, Correlation and Euclidean Distance). The results indicated that when using multilevel thresholding aggregating contextual information with Object-Oriented refinement by Scale descriptor and application of Low Pass Filter by Mean Convolution, there is significant improvement in results. Was possible to assess the quality of the method and its feasibility for remote monitoring in agricultural production, where the model can be used as a significant indicator of oscillation and multitemporal trends in the use and land cover. Thus, the PV Model can facilitate inspection by of the countries with subsidies for agriculture, whether by inspectors from the Government or by Financial Institutions, in addition to reducing costs in the operational process concentrating face-to-face visits only for areas of large hectares.*

I. INTRODUCTION

Globalization and technological advance have caused changes in the way Organizations. In the competitive and volatile scenario, where information is essential for strategic decision making, it is increasingly necessary to use tools that allow an efficient management of information, helping in the extraction of data and intelligent decisions.

In this scenario, the use of geotechnologies has contributed to a continuous and agile monitoring of the reality in society, acting in monitoring such as in the use and cover the land with the Agribusiness, which is one of the main sectors of the world economy. The agriculture is one of the main responsible for the positive balance of trade in several countries, and the sector is fundamental to the economy of developing countries [5] [43].

In the last years, the world population has been growing exponentially. Thus, it is necessary to optimize and improve the production process, for the better use of inputs, with investments in technology and better cultivation practices, because with the population increase greater demand for food will be necessary. Although, there are few countries that still have uncultivated areas that can be used for agriculture, where 90% of them in Africa and South America [1] [4] [57] [59] [73].

Considering the countries that have uncultivated areas that can be used for agriculture, a lot of do not have technologies for production and the lack of qualified professionals and economic resources. Therefore, within the perspectives and scenarios, the Brazil is an important global producer to supply as business opportunities and the production supply of food in the world. The country concentrates around 14% of the world's fresh water, has a diversified climate with regular rainfall and only 34% of its area is used in agribusiness. It's one of the main producers of agricultural commodities in the world, the 4th largest grain producer and the agribusiness represents an growth in the economy with Gross Domestic Product (GDP) next to 25% [1] [17] [21] [22] [51] [64] [69].

Thus, as different countries, such as Egypt, Morocco, Nigeria, Japan, France, South Africa, among others, have government policies with incentives for agricultural financings, in the Brazil is not different, either by the importance of the sector in the economy whether due to the surplus in the balance of trade or inflation control. The most countries have government incentives in the sector through agricultural credits released by Banks and Financial Institutions. This rural credit is financing for rural producers whose activities involve the production and/or sale of products in the agricultural sector. Soon it is necessary to have risk mitigators in the financeable area in order to monitor agile and efficient manner the reality of agricultural areas, where many of the agricultural practices end up having financing through the National Financial System of countries sponsors. Thus, the use of geotechnologies helps with this monitoring in an agile and transparent way [1] [60] [73] [82].

For example, the Brazil Central Bank (BACEN) recommended that Banks and Financial Institutions, with rural credit operations, use the Remote Sensing to contract and inspect agricultural operations credit operations. According to Resolution, since 2016 the use of GISs (Geographic Information Systems), satellite images, photogrammetry or data obtained through RPAs (Remotely Piloted Aircraft), commonly known as Drones and UAVs (Unmanned Air Vehicles), is authorized to monitor agricultural financings and evaluate of the vegetative development in each phase of crop cultivation, recording the initial, full and final stages of vegetative development. In general, the countries have inspection methods are almost entirely in loco, which makes monitoring costly and often with only reactive actions [7].

One of the main applications of Remote Sensing is in detecting changes in land use and land cover. Through the analysis of a series of satellite images, with acquisition at different times, a comparison is made in the areas of interest in order to identify what, where and how much was modified in the study regions, through the spectral responses of the targets [74] [78].

Considering the context presented, the objective of this study was to propose a method of detection of changes in agricultural areas, by an open source tool with automated emission of messages for the cases in which a change in behavior is detected. Thus, a tool in Python language was developed, called LimiariZC, where was developed modules and built the model that was called Peaks and Valleys, using multi-level thresholding in histograms and analysis based on objects. In this way, with the model are possible risk mitigators of the financeable area and remote inspection instead of in loco, reducing face-to-face work to monitor the development of cultures, analyzing the vegetative cycle of the crops by remote. The model was applied in a study area in Brazil but can be used in any region of other countries for monitoring areas with agricultural financing or that will be financed and thus have greater control and transparency.

II. THEORETICAL REFERENCE

2.1 Multilevel Thresholding

The segmentation is based on two characteristics relative to the shades of grey of an image: discontinuity

and similarity. The discontinuity method considers the abrupt change of gray values and the similarity method is based on the aggregation of pixels according to their similarity to neighboring pixels. Among the types of segmentation based on the similarity feature are the methods of segmentation by region growth, thresholding, basin and pyramid detection. In thresholding segmentation, a discretization of objects by thresholds is made over the image histogram, where segmentation in conjunction with digital processing enables temporal detection of changes. Thus, the segmentation algorithms, at an early stage, contribute to reducing the complexity of classifications in the detection of changes [14] [48].

Multi-level thresholding, or multilevel segmentation, can be defined as an extension of two-level segmentation methods, with the difference that it enables segmentation into multiple classes. Thus, its use is recommended when you have several objects in the scene that differ from the background. The presence of the various objects makes the gray level distribution histogram multimodal, where the segmentation threshold is found by the location of the valleys separating each of the objects into classes [79].

For [58], in a macro way and considering the evolution of the methods over the years, there are two classical methods of thresholding which were derived from the others. The first was the one proposed by Otsu [61], which aims at maximizing the variation between classes to find the optimal separability threshold. The second was the one presented by Kapur [42] that uses entropy maximization to measure homogeneity between classes. Both methods are efficient and precise for unimodal segmentation, that is, with two levels and presenting two classes. However, although the methods can be expanded to a multi-level threshold, the complexity and computational performance of the methods is exponentially intrinsic to the addition of new levels, making the process costly.

In recent years, different models have been proposed in order to foster the academic area with multi-level thresholding, aiming at improving the limitations of the methods presented by Kapur and Otsu [42] [61] for bimodal histograms, such as the work of [81] which uses the weighted variance of objects for detection. In [47] a recursive algorithm for multilevel thresholding is proposed, where the proposed algorithm demonstrates performance improvement over the original method. The study brings an approach that aims to maximize the variance between classes, the calculation of accumulated probability and moments of zero order and first order.

For [32] brings a hybrid approach to multilevel thresholding using the Otsu method and adjustments to the Gaussian function. The algorithm called Nelder-Mead (NM-PSO-Otsu) demonstrated that it improved the results presented through the original method. However, most models bring mathematical and computational complexity.

According by [71], thresholding methods can be grouped into six categories, according to the use of detection techniques, and they are based on histograms (focusing on the analysis of peaks, valleys and smoothing of curvatures), clusters (where gray level samples are grouped in parts separating the object from the background), entropy (where the algorithms use entropy to separate the regions between the objects and the background), in object attributes (where the similarity between the gray level and the binary images is measured, as in fuzzy similarity), in spatial methods (where they use the highest probability of distribution, as well as the correlation between pixels) and in local adaptive methods (where they consider the local value of each pixel).

Although there are different thresholding methods, those based on histograms are simple and quick to perform, as in general the logic of the technique is that pixels assume a categorization according to a defined pattern, and those that do not fit this label remain in another category. In general, in histogram-based methods, thresholds are selected based on the analysis of thresholds that promote the best separability of classes, adapting the Otsu method and using Gaussian models [11] [36] [55].

In a macro way, histogram-based thresholding techniques can be classified on two fronts. The first with thresholding techniques that determine the ideal thresholds, optimizing a certain objective function [33] [50] [80], where approaches based on entropy such as Shannon, Renyi [3] [67] [72] entropy correlation and cross entropy [68] can be found. However, the main associated obstacle is the high processing time. On the second front, there are techniques that seek the optimal thresholds through the form of histograms, where it is assumed that the intensity of pixels is similar on the same objects and distinct on different objects [50].

The proposed work reflects a multilevel threshold that can be applied to any type of histogram and aims to verify in an automated way whether or not a crop has been harvested. Thus, the model assumes that when there is a vegetation cut, becoming exposed soil in the satellite image, the response in the histogram would present a different gray level value for the region, compared to the same location in the histogram of the image at the previous time, displaying a valley instead of a peak and vice versa. The same occurs for vegetation, where it would present a higher frequency compared to the exposed soil.

2.2 OBIA - Object Based Image Analysis

The process of image classification allows, besides the identification of targets in satellite images, quantitative analysis of objects of interest in the scene, such as studies of the evolution of the environment, calculation of areas, among other factors in the detection of patterns and monitoring of behaviors. The process of extracting the information in the images is performed through classifiers, which have mathematical methods that directly assist in the stage of the classification process. Most methods are based on the attributes of tone, color and texture of the targets. One of the classifiers divisions is the main unit of analysis, being defined in classifiers per pixel and per region [18] [52].

The classifiers per pixel operate with the attributes of tone and color, as is the case of the classifiers of Parallelepiped, Euclidean Distance, Maximum Likelihood among others. The classifiers by region, on the other hand, in most cases work with the aspect of color, tonality and texture, like the Isoseg and Bhattacharya classifiers. While pixel by pixel classifiers use only the isolated spectral information of each pixel, those by region, besides the spectral information of each pixel, make use of the spatial information that involves the relationship between the pixels and their neighborhood. Thus, in region classifiers, it is necessary to use the segmentation technique to fractionate the image into regions with similar responses [14] [48].

In high spatial resolution images and in classifications where the spectral response of the targets is similar, the classifiers per pixel and per region may not perform efficiently. In such cases, the use of object-based classification becomes more satisfactory as a result of these types of classifiers using, in addition to hue, color and texture, other characteristics pertinent to the image, such as shape, location, size or scale among other attributes of the target of interest in the scene. In object-based classification, the region of pixels is called the object, and the characteristics of the objects are used in the classification decision. For the generation of objects, segmentation is required, where the user uses the object attributes in a decision tree for the classification [10].

Object based classifiers are based on the GEOBIA (Geographic Object Based Image Analysis) system, also known as OBIA (Object Based Image Analysis). Such classifications refer to a knowledge-based analysis, with automatic image interpretation, through Object-Oriented data analysis. Instead of the classification being performed only in isolated pixels - being pixel by pixel, without considering the neighborhood - it uses as parameter the segments or set of pixels. Therefore, it considers geometric particularities of the targets, such as area or scale, color, dimension, texture, format, proximity of segments, among other particularities and refinements. Thus, it not only uses spectral, but also structural and spatial characteristics in the process of class distinction [12] [56].

According by [31], the OBIA approach brings an advance in automatic classifications of orbital images, where it allows a better discrimination of features in high resolution images. Because it has less influence on the spectral mixing of targets, it automatically distinguishes the gray levels of the image, when compared with conventional classifiers. Because it is knowledge-based analysis and has less human intervention, automatic classification is close to reality in the field.

The GEOBIA paradigm consists, in a macro way, of the segmentation and classification steps. Segmentation defines the division of the image into groups with homogeneous characteristics taking into account factors defined by the operator, such as compactness, scale and smoothness. The classification is based on the definition of decision rules that reveal the properties of objects expressed by their attributes. Thus, the classification based on objects allows a better discrimination of features in high resolution images. Because it has less influence on the spectral mixing of the targets, it better distinguishes the grey levels of the image [14] [52] [54].

In the proposed method, the Peaks and Valleys Model (PV) was implemented, where it brings a multi-level thresholding approach by aggregating object-oriented (O.O.) contextual information. Through the extracted thresholding, the classification of the detected segments will be performed, which will be refined based on objects by the Scale descriptor, besides the context analysis of the segments through the extraction of the Entropy parameters and the Homogeneity and Correlation texture descriptors. In addition, the attributes of Euclidean Distance between the segments will be used, as well as the extraction of statistical parameters of Mean, Standard Deviation and Coefficient of Variation (CV). The descriptors extracted were intended to verify the behavior of the attributes before and after the O.O. refinement and before and after the application of the filter in the histograms, in order to verify if the OBIA information and the use of filter aggregated to the multilevel threshold promotes improvement of the results.

The Scale attribute used in OBIA refinement will be used to delimit the dimension of each object found. Through the parameter, the heterogeneity regarding the size of the objects will be checked. The larger the delimitation of the scale value, the larger the size of the regions generated. From the input parameters, defined by

the user in the tool developed, it will be possible to define the minimum percentage of area that each segment has, based on the total pixels of the image. If the object has a number of pixels lower than the determined percentage, the class will be grouped next, forming clusters according to the established definition, so that all classes have the minimum percentage of pixels stipulated, refining the segmentation for the effective recognition of patterns. The scale factor value may vary from zero to a user-defined finite value [6].

Entropy reflects the randomness of the image data, since the more dispersed the data, the higher the entropy values will be. Thus, the value reflects the impurity of the data, that is, the lack of homogeneity between the information [70]. The proposed method applied Shannon's entropy [72], which quantifies the information and measures the degree of uncertainty and can be used in the characterization of textures [9]. For the attributes of Homogeneity and Correlation, Haralick's descriptors [30] were used, which determine texture characteristics of the selected images. Homogeneity is a spatial autocorrelation measure representing the distribution of pixels along the cluster and/or image. The descriptor assumes high values when the texture presents small variations of gray levels, with a range from 0 to 1 [30]. In the Correlation, it is possible to analyze the similarity between the segments by means of the mean and standard deviation values, where the measurement allows verifying how much a pixel is correlated with its neighbor. Thus, the texture correlation measures the linear dependence of pixels in relation to their neighborhood. The comparison is performed on all pixels of the class and returns the average value to the cluster. The descriptor has values ranging from -1 to 1, where when an image or class has the pixels fully correlated, the value obtained is 1. When they are fully correlated, the value is -1 [30]. While the descriptors mentioned reflect the intra-cluster quality, the Euclidean Distance represents the inter-cluster separability, that is, it represents the geometric distance in multidimensional space, and the higher the value of the distance calculation, the less similar - or more dissimilar - the objects will be. Therefore, the smaller the value of the distance, the more similar the analyzed regions are. Thus, the distance between class ranges is expected to be the greatest possible, indicating the good separability of clusters [19].

The statistical parameters of Mean, Standard Deviation and CV are measures of dispersion that indicate the regularity of a data set, being possible to analyze the oscillation around the mean. The smaller the deviation, the closer the values are to the mean and the bigger, the more distant the values are from the mean. Thus, through the variables it is possible, for example, to check the mean of the objects that belong to a certain cluster and analyze if the pixels are close to each other or vary significantly. Also, the smaller the CV value found for the clusters, the more homogeneity there will be in the data [15].

Through the analysis of the extraction results of the attributes in the images, the knowledge model will be defined so that rules can be established for the detection of seasonal changes in the bi temporal analysis of the scenes, so that the multitemporal monitoring of changes can be performed.

2.3 Change Detections

There are different techniques for detecting changes through multitemporal image analysis developed in recent years, and there is no universally accepted method [20] [74]. The parameters of choice of these techniques depend on the objective of the research, as well as the preferences of the operator in the use of certain tools. In a macro way, the techniques of change detection can be grouped in five modalities: ratio between bands, difference between bands, analysis of main components, temporal spectral classification and comparison of individual classifications [39].

According by [28], the techniques of band ratio, subtraction or difference of image bands and main components are the most used for the detection of changes, being able to monitor changes in the spectral response pattern of vegetation as a function of time, either due to phenological changes of plant species or by anthropic interventions.

Among the approaches to detect change is pixel analysis, with studies from urban development [76] to changes in land use coverage [63]. However, the use of pixels as comparators of change is not an adequate approach when using high-resolution images, mainly because of the lack of contextual information for decision making and only pixel tonality or radiation [16] [34]. Furthermore, such detections are susceptible to noisy classifications with the so-called "salt and pepper" effect when considering only the pixel [8] [12] [16].

The task of distinguishing objects in an image, in a digital way, can be extremely exhaustive, requiring very elaborate filters and reaching very efficient results. However, requiring a high quality in the detection of changes, usually also requires a high price, that is, the algorithms have now high cost, high mathematical and computational complexity, high specificity and low robustness. In order to meet the requirements in a timely manner, digital image processing systems use, at a primary

stage, segmentation to highlight the background object [41] [53] [75].

A statistical trend analysis was proposed in order to complement the automated histogram sweep in search of thresholds in order to minimize possible false positive and/or negative alert emissions. The trend analysis aims to verify if the change occurred between the pair of scenes is due to loss of vegetation or vegetative growth.

The rules for emitting the flags were implemented by means of a decision tree proposed and developed in the tool created, considering a set of variables and descriptors of first and second order extracted from the base of analyzed images, where a spatial analysis of the objects will be carried out in order to evaluate if there were changes or not. Traditionally, decision tree algorithms, such as J48 [29], Random Tree [83], Random Forest [83], REPTree [83] and Logistical Model Trees or LMT [45], start from a set of chained rules forming a hierarchical structure similar to a tree. In J48, each node of the decision tree is assigned an attribute that best subdivides the classes into homogeneous sets, where the tree pruning criterion is used so that the search is not extensive. In Random Tree, a random quantity of attributes is considered at each node, without pruning the decision tree [27]. Unlike the others, in Random Forest the objective is the generation of several decision trees by means of randomly selected attributes, the chosen attributes being called bootstrap where there is replacement in the samples in order to improve the interpretation of data, forming new subsets that will constitute the decision tree [49]. In REPTree the decision tree uses information of gain and variance, where the values are changed according to the pruning aiming at error reduction [27]. Finally, the LMT algorithm aims the generation of trees through logistic regression, where the objective is to select relevant attributes in the data set through repetition [25].

In the study presented by [40], different classification algorithms based on trees were evaluated to select attributes in order to avoid cyber attacks, where Random Tree demonstrated the best predictive accuracy, with fewer false positives/negatives among the evaluated algorithms. In the analysis made by [37], Random Forest obtained 82% accuracy in the classification of ten tree species through WorldView-2 images in a study region located in eastern Austria. Although the algorithms have expressive results in several areas for data mining and pattern recognition, it was chosen to create the native tree of the proposed method through the attributes of statistical trend analysis for the emission of signals in the monitoring of alerts/warnings, because the analyzed data indicate a common behavior to express the trend. Thus, in the empirical model generated, the set of descriptors should be considered as attributes to direct the hierarchical tree, without the substitution of the parameters by the repetitivity employed in the traditional decision tree algorithms, aiming at finding the best separability attribute.

III. MATERIALS AND METHOD

3.1 Study Area and Materials

The study area is concentrated in the eastern portion of the Federal District (DF) around the region called PAD-DF, Federal District Directed Settlement Program, near the border of the state of Goiás in the municipality of Cristalina between latitude -16.09815 and longitude -47.47153 encompassing an area close to 70 hectares (ha), as shown in Fig. 1.

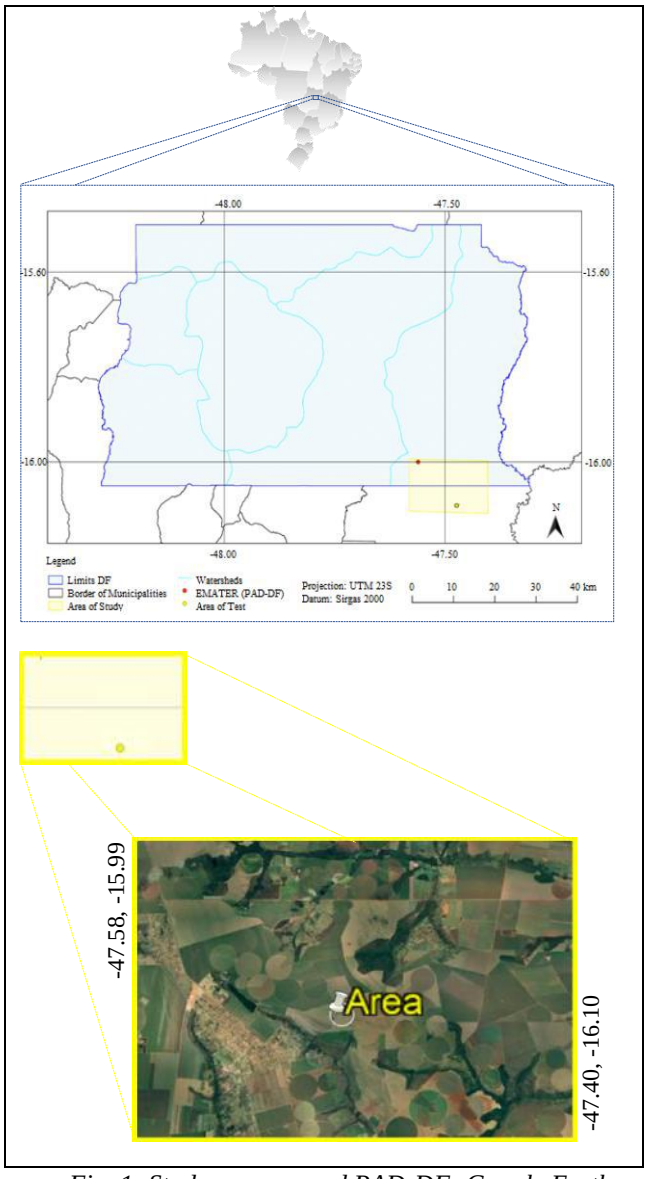

Fig. 1: Study area around PAD-DF: Google Earth image from April 10, 2020.

The polygon was chosen because it visually presented different nuances in the plot, which could represent different classes in the images and consequently multimodal histograms for the scenes. According to the field visit made in the property in 10/23/2019, in the plot there is the diversification of Horticultural crops. Thus, detailed tests were applied to the polygon in order to analyze the effective applicability of the tool developed in the distinction and separability of thresholds or classes of images. According to data from the Brazilian Agricultural Census and land structure [35] [38], of the total 6.5 MM of rural properties in the country, about 86.5% have less than 100 ha. Considering the DF dimension, the value rises to 94.3%. Thus, the size of the study polygon covers the largest quantity of rural properties.

The PAD-DF is a program implemented in 1977, with the intention of occupying large areas of the Brazilian Cerrado with agribusiness. The program arose from the need to offer an economic and agricultural destination to the areas of the Brazilian Cerrado in the Federal District, at a time when research initiatives and incentives for agricultural activities were emerging. Thus, it covers an area of over 60 thousand hectares, containing several types of economic initiatives, from areas with cereal plantations, horticultural crops, cattle farming, poultry farming among others, through producer settlements in isolated areas, rural nuclei and agricultural colonies, and in the region some of the main agricultural crops produced in the Brazilian Cerrado are found, such as soybeans, corn, wheat, cotton, beans, onions, potatoes and carrots [13] [26]. According to Table 1, nine Nanosatellite Planet images were used for monitoring the agricultural development cycle.

Table. 1: Images used for monitoring of the culture development cycle.

Imagery Date		
Nov 14, 2017 (Time: 12h45'10''; % cloud: 0%)	**Nov 28, 2017** (Time: 12h43'58''; % cloud: 0%)	**Dec 28, 2017** (Time: 12h45'48''; % cloud: 0%)
Feb 14, 2018 (Time: 12h48'00''; % cloud: 0,16%)	**Apr 27, 2018** (Time: 12h50'43''; % cloud: 0%)	**Oct 04, 2018** (Time: 13h39'52''; % cloud: 0%)
Jan 03, 2019 (Time: 12h52'13''; % cloud: 0%)	**Jan 15, 2019** (Time: 12h58'38''; % cloud: 0%)	**Feb 02, 2019** (Time: 12h58'55''; % cloud: 0%)

The Planet images were defined as the scope of this work by the imaging characteristics of the nanosatellites, with a significant daily and spatial resolution of 3 meters, allowing the traceability of the plots with agricultural financing in an agile way, being fundamental for monitoring the vegetational cycle of crops. Thus, as the images are made available almost instantly when captured by the sensor system, if any abnormality outside the standard is detected in the automated monitoring proposed by the tool, it is possible to adopt timely actions in an agile and effective manner, such as, for example, on-site inspection for cases where some inconsistency was actually detected. Thus, it was adopted as a premise that the better the spatial temporal resolution the better the monitoring.

The analysis and selection of images were based on the criteria of scene availability, dates based on the phenological periods of the crops present in the plot, non-existence of clouds and visual inspection that indicated significant seasonal changes in the scenes, aiming to find periods with greater contrasts to evaluate the differences and consequently apply and validate the proposed method with assertive signs for the crops. The images used are the Ortho Scenes level 3B, which are made available by the supplier with geometric, radiometric and orthorectification corrections, in addition to being made available georeferenced, normalized and scaled with Radiance in the Top of the Atmosphere (TOA), being delivered in the analytical products for the 4 bands (R, G, B, NIR) [65].

Envi 4.8 and QGIS 2.18 applications were used to cut out the plot on the images and validate the accuracy of the classifications. However, the execution of the method proposed and implemented in the tool is independent of the use of other software. All processing was performed on a microcomputer with Intel I-7 processor, with processing speed of 2.8 GHz, RAM of 16GBytes, HD capacity of 1 TByte, SSD 224 GBytes and Windows 10 operating system.

3.2 Methodological Approach

The methodological procedure was divided into three stages, as shown in the Fig. 2.

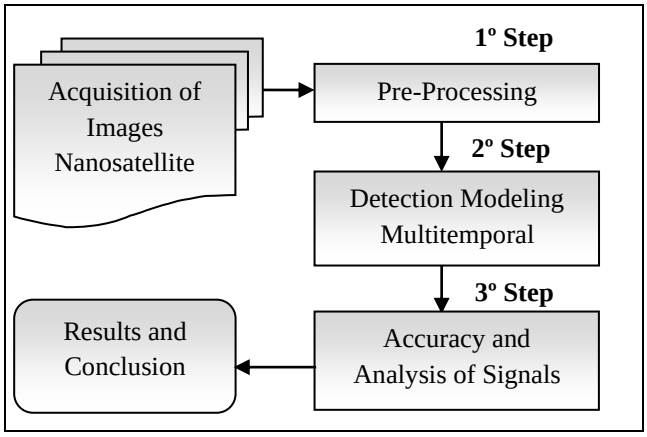

Fig. 2: Macro flowchart of Methodology.

3.2.1 Methodology – 1º Step

In the first stage the pre-processing of nanosatellite images was carried out, with the selection and clippings of the study areas, as well as the necessary treatments in the scenes for the complete effectiveness of the proposed method. In this way, in the clippings of the areas, masks were created to delimit only the plot of interest, besides the conversion of the scenes to 8 bits. After several tests, the conversion of the images was chosen to improve the performance and optimize the processing time in the execution of the models, besides minimizing the existence of short peaks and shallow valleys in the images.

3.2.2 Methodology – 2º Step

In the stage, a Multitemporal Detection Modeling was developed. The proposed method was implemented, in Python language, through the development of a tool, called LimiariZC, where a multilevel thresholding model called Peaks and Valleys (PV) was developed, with the objective of to propose a method for detecting changes in agricultural areas, with automated emission of messages for cases in which behavior change is detected. In the model, an automated histogram scan is performed in order to find the location of peaks and valleys in any type of histogram. The model aims at verifying if in a certain location the crop continues with the evolutionary growth according to the standard behavior or if there are signs of crop cutting or vegetation loss. In this way, it is possible that images are compared to pairs performing a bi temporal seasonal detection, from pre-planting to harvesting, passing through the different phases of cultivation.

In the Fig. 3 shows the macro task flowchart of the PV model developed in the change detection tool.

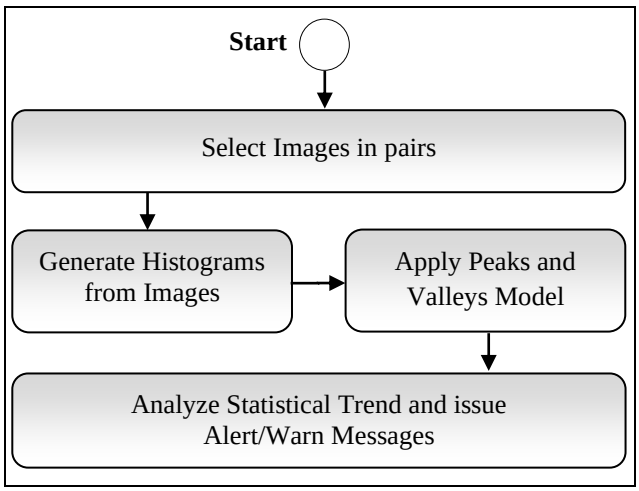

Fig. 3: Macro flowchart of the Peaks and Valleys Detection Model.

For each of the input images, the corresponding histograms are generated. In order to attenuate the short peaks and shallow valleys in the scenes, generating classes with a small number of pixels, it is possible to apply in the PV model low-pass convolution filter of the medium type in the histograms, besides an object based refinement by the Scale descriptor which agglutinates the classes according to the minimum percentage customizable considering the image dimension, forming clusters according to the established definition. With the application of the model, the statistical trend of the scenes is evaluated, emitting - according to the rules defined in the proposed decision tree - messages of vegetation loss alerts or vegetative growth warnings.

3.2.2.1 Peaks and Valleys Model

The purpose of the model is to search for the valleys in the image, that is, the places where the thresholds of separation of the scene classes from the grey level of the pixel are concentrated. In this way, if there is a valley, a threshold will be detected, and the image will be segmented through the threshold. The automatic thresholding algorithm developed allows the detection of the valleys through the signal transition of the histogram values, where every time there is a signal transition from negative to positive it indicates the position in which a valley is located, therefore, a new threshold and a possible new class. Each of the segments, delimited by the thresholds, comprises a new region fragment with homogeneous units. In this way, a monitoring is performed throughout the histogram in order to find the separation thresholds.

The Peaks and Valleys detection algorithm is executed according to the listed tasks:

1. For each histogram, the algorithm acts as if it divided the histogram into sub-regions or rectangles;
2. For each of the sub-regions the corresponding areas will be calculated;
3. For each one of the histograms, a resulting vector shall be created;
4. For each corresponding resulting vector, the result of each area calculation of the sub-regions will be stored;
5. In the resulting vector, automated searches will be performed verifying the signal transition between the elements (thresholds);
    - ✓ If there is a transition from negative (-) to positive (+) sign, it indicates the position where a "valley" is located;

- ✓ If there is transition from positive (+) to negative (-), it indicates the position where a "peak" is located;

6. After all thresholds in the image are detected in the resulting vector, each threshold interval will be associated with a class. Thus, the cluster of pixels located in a given threshold range will be part of the same class;

7. Through object-based analysis, the thresholds (or segments) can be refined by extracting attributes, using the Scale descriptor. The values of the parameters will be defined by the user, where the tool developed allows the customization of the parameters by the operator, according to the analysis of the input scenes;

8. In the resulting vectors, comparisons will be made between the stored thresholds for each one of the histograms, as well as analysis of statistical tendency in the images, aiming at finding changes in behavior from one analyzed image to another;

9. In case of detection of behavior changes in the different phases of the evolutionary cycle, according to the maximum percentage range of oscillation defined by the user and the statistical trend analysis, alerts/warnings will be issued by the developed tool.

The area calculation of each sub-region, containing the signal transitions, will be implemented through the mathematical model in Equation 1:

$$A_n = [(X_{n+1} - X_n)(Y_{n+1} - Y_n)] \qquad (1)$$

Where An is the nth area calculation of the sub-region, n is the pixel position of the analyzed image, X_n the abscissa of the nth gray level and Y_n the ordinate of the nth gray level.

In the sequence, the values are stored in a resulting vector. Subsequently, the resulting vectors of each of the histograms are compared to each other for further classification. The vectors are analyzed to monitor possible class changes in the study areas, and detection is performed on each of the input images. The resulting vector, containing all calculations and signal transitions for the input images, is given by Equation 2:

$$V_{Result} = [A_0, A_1, A_2, A_3, \ldots, A_n] \qquad (2)$$

Where V_{Result} is the vector containing all the results of the subregion calculations, concentrating all the signal transitions and the result of the area calculation, from the first to the n-th pixel of the image.

In Fig. 4, the proposed modeling for searching peaks and valleys is exemplified in the histogram of each input image. For each subregion of the histogram, each position of the pixels corresponding to the pair of coordinates (x, y) is monitored. Area calculation is performed for each of the segments, and the result is stored in the resulting vector of each histogram. Thus, there will be a resulting vector for each image analyzed, concentrating in each vector all the signal transitions of the calculations. The resulting vectors are compared among themselves, aiming at identifying, from a pre-established range, if the behavior of the resulting vectors is similar to each other, issuing warnings in cases of deviations from expected behavior. Thus, it is as if the input images obtained in different periods were being compared among themselves, aiming to identify behavioral changes.

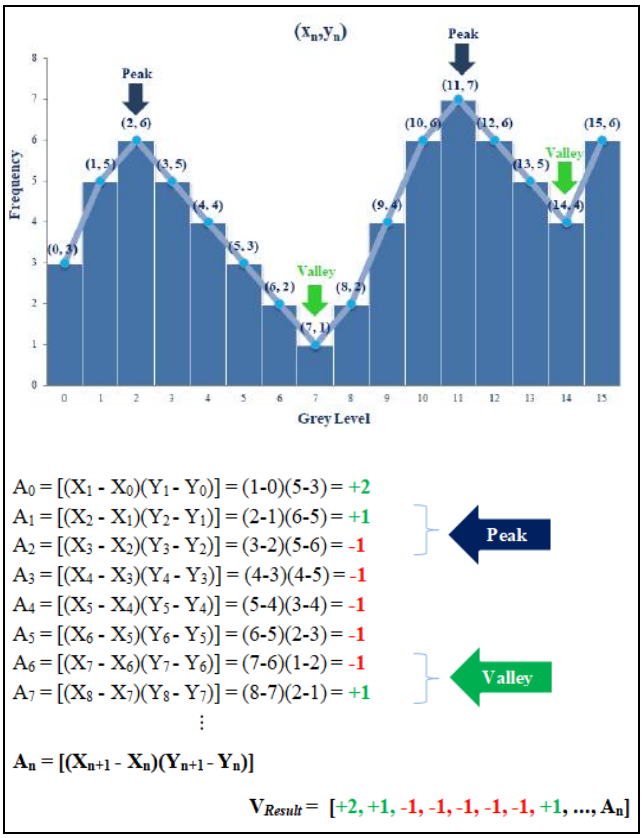

Fig. 4: Modeling proposed in the Model of Peaks and Valleys.

Mathematically, the automated scan in the histograms, is performed as if the intention was to obtain the maximum and minimum points of a polynomial function. Thus, for a histogram with known polynomial degree, if the mathematical calculation of the first and second derivation was performed, it would be possible to discover the inclination of the tangent line to an f(x) function and thus find the points of minimum and maximum of the curvature [23]. However, the automation process is not trivial, since it should be customized according to each histogram because the function f(x) is not always the same. This is

due to the fact that there is no standard polynomial behavior due to the shallow peaks and valleys in the image histograms. Thus, as for each image the degree of polynomial is different, the solution proposed in this article is the implementation of the algorithm that performs automated scanning, in search of the points of abscissas and ordinates in which there is the signal transition between peaks and valleys. If the comparison of detected thresholds or valleys is different in the pair of images analyzed, it is a strong indication that there were changes between the scenes, otherwise the quantitative would be equivalent.

3.2.2.2 Statistical Trend Analysis and Alert/Warning Emission

Based on the different images and tests applied, an exploratory analysis of the data was performed in order to characterize the behavior of the possible classes involved in the study for multitemporal detection modeling. Statistical trend analyses were performed in order to identify the spectral behavior of each of the growth and vegetation loss patterns, in order to obtain the spectral response of each of the targets and thus be able to complement the warning emission of the peak and valley model, in order to avoid false positives and/or negatives of vegetation loss. After the extraction of different first and second order statistical parameters, it was found that the attributes listed in Table 2 could be assertively used for detection of the vegetation (VEG) or the loss of vegetation with the presence of the exposed soil (E.S.).

Table. 2: Statistical Trend Analysis for the Emission of Signalizations.

	ALERT	**WARNING**
VARIABLES	**I1 = VEG and I2 = E.S.**	**I1 = E.S. and I2 = VEG**
Mean	I2 > I1	I2 < I1
Entropy	I2 > I1	I2 < I1
Standard Deviation	I2 < I1	I2 > I1
Maximum Peak Frequency	I2 < I1	I2 > I1
Coefficient of Variation with Homogeneity Analysis	ΔCV < 0 H < 0	ΔCV >= 0 H >= 0

Thus, according to the statistical criteria analyzed, in the seasonal bi-time analysis between the scenes, an alert or warning signal should be issued for the monitored area. The warning message will be used to signal possible loss of vegetation while the warning message will be used to indicate vegetative growth trend. Through statistical trend analysis with the proposed attributes, a native decision tree was created in the tool for issuing the flags.

3.2.3 Methodology – 3º Step

In the 3rd stage the analysis of the Alerts/Warnings emissions was performed by visual interpretation of the input images, aiming to evaluate the implemented model of automated change detection. The results were compared in order to verify if visually the signals, in fact, should be issued and/or if in the assessment areas there were signs of some undetected, in order to avoid false positives and/or negatives. Thus, the agricultural areas of the multitemporal application were individually analyzed, being evaluated by means of the keys of interpretation regarding color, shape and texture [24].

IV. RESULTS AND DISCUSSIONS

The Fig. 5 shows the monitoring for the vegetative cycle of the stall from initial, full, maturation to cutting. For each image comparison, the statistical trend analysis is extracted, informing by means of signs the trend of the stall: if of warning of vegetative growth or alert of vegetation loss.

The proposed and developed method takes on average 25 seconds to process areas up to 100 ha. As can be seen in Fig. 5, the alerts and warnings issued were assertive in all tests, where it can be ratified by the visual comparison of the images with the different nuances of exposed soil and vegetation. Thus, it was verified that in the bi temporal analysis between the pair of images, when there are changes in vegetation nuances, indicating greater vegetative vigor in the most recent scene, a warning message of vegetation growth was issued, according to the transitions on 11/14/2017 and 11/28/2017 (Cycle 1), 11/28/2017 and 12/28/2017 (Cycle 2), 12/28/2017 and 02/14/2018 (Cycle 3), 10/04/2018 and 01/03/2019 (Cycle 6), 01/03/2019 and 01/15/2019 (Cycle 7) and 01/15/2019 and 02/02/2019 (Cycle 8).

On the other hand, in the biennial analyses of 02/14/2018 and 04/27/2018 (Cycle 4) and 04/27/2018 and 10/04/2018 (Cycle 5) the loss of vegetation is clear, indicated by the presence of exposed soil on the scene. Thus, an automated warning message of vegetation loss tendency was issued based on the decision tree developed.

Still analyzing the results presented in Fig. 5, in the Cycle 5 images although both scenes indicate the presence of exposed soil, the most recent image (04/27/2018) appears lighter and closer to white nuances indicating less vegetation remains compared to the older image (10/04/2018). Thus, the message of the warning of vegetation loss was flagged, indicating that the proposed method in the PV Model was assertive even for exposed soil transitions.

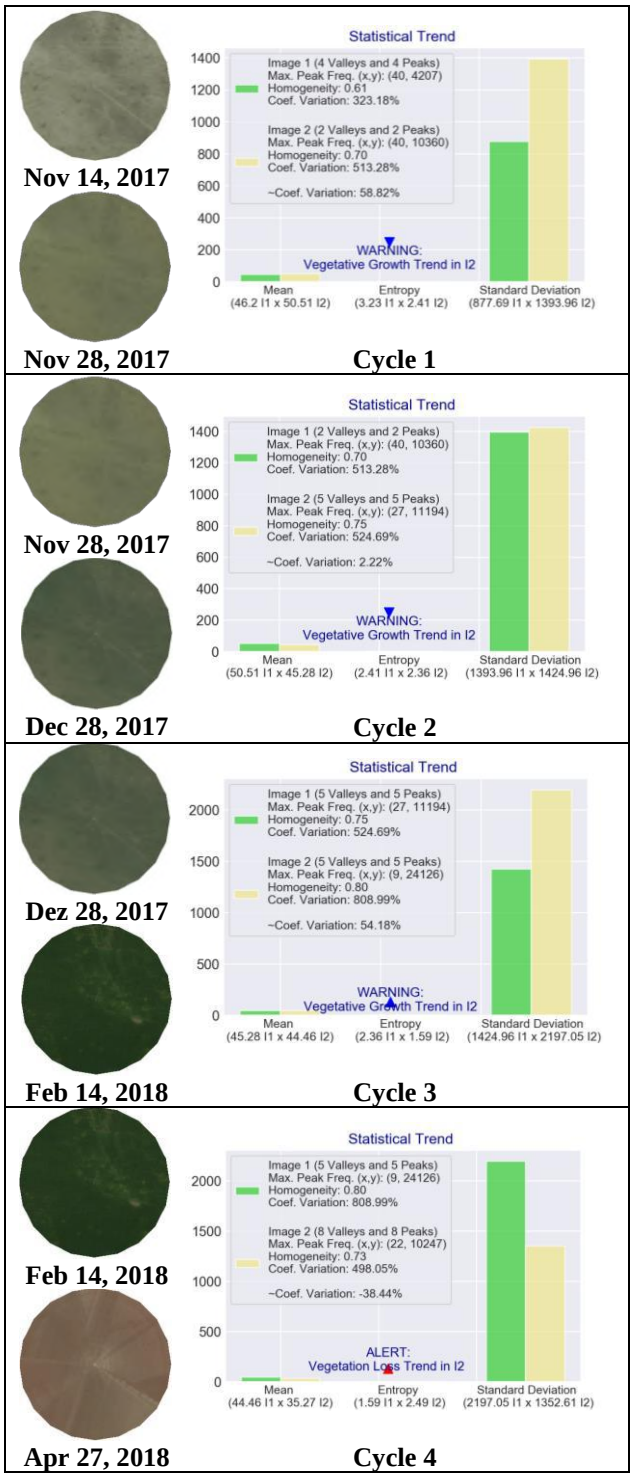

Fig. 5: Vegetative cycle of the plot, from initial, full, maturation and cutting.

For the images of the area that succeeded the pre-planting, in the scenes of 01/03/2019, 01/15/2019 and 02/02/2019, representing Cycles 7 and 8, vegetation growth alerts were issued for the evolution of the initial vegetative cycle, full and maturation, according to the analysis of statistical trend performed. With the effectiveness of the alerts and warnings issued in an automated way, the accuracy of the threshold

classifications obtained in the tool was verified, according to Fig. 6.

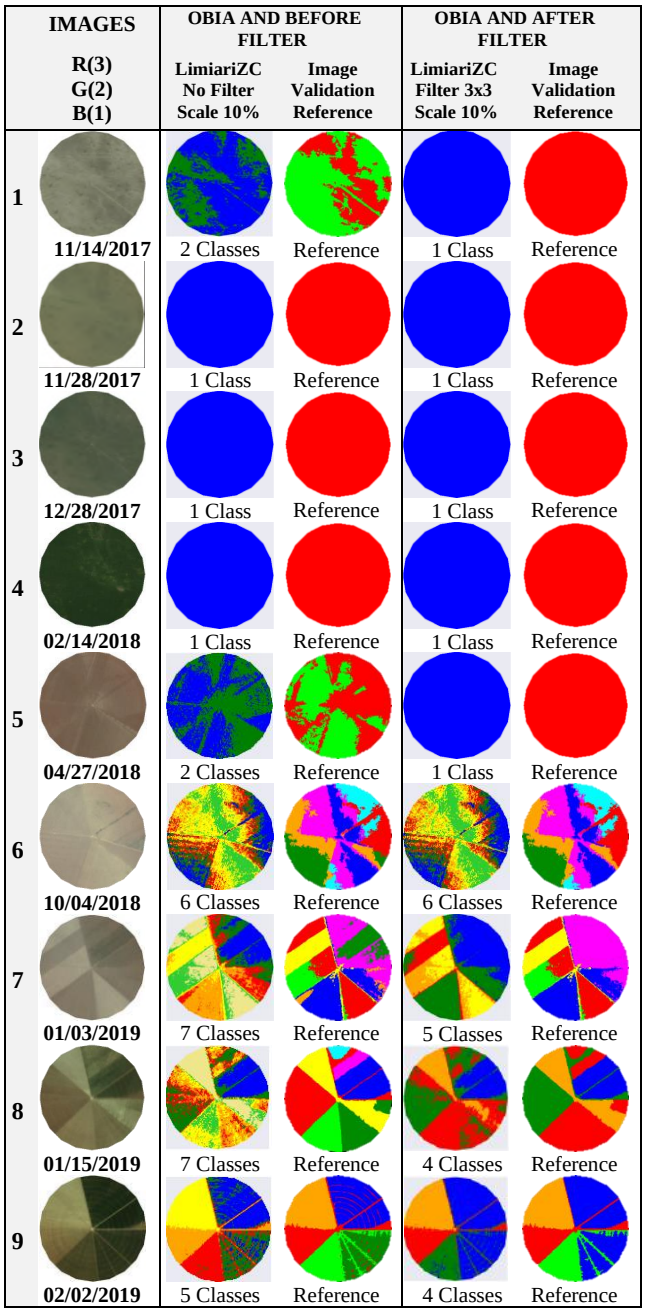

Fig. 6: Classifications extracted with the respective validation reference.

The validation of the classifications was performed by adopting as reference image the classification by visual interpretation, such classification being adopted because it acts in a proportional manner to the thresholding logic, where the visual interpretation, by means of screen digitalization with vectorization of the image, allows aggregating in a polygon the pixels with visually similar characteristics. Thus, in the PV model the groupings are formed based on the valley, which represents the gray tone with the lowest value in the histogram and separate similar regions based on the proximity of gray level. Thus, studies show that when the visual classification is used as a reference map of the actual scenario, it allows the decrease of the classification error with consequent increase in overall accuracy [66] [77].

Fig. 6 shows the analyzed input images with the respective threshold classification generated with OBIA refinement by 10% Scale, before and after the application of the filter passes low average convolution with 3x3 dimensions, besides the reference image used in the validation. The accuracy was extracted for the images with OBIA refinement and the use of the filter due to the application of the descriptors demonstrating that this is where the results had better quality in the groups.

For all the bimonthly analyses performed, the descriptors of Entropy, Homogeneity, Correlation and Euclidean Distance of the scenes were extracted in order to verify the behavior of the attributes before and after the O.O. refinement and before and after the filter application. The tests indicated that when the filter is applied to the scenes and the multilevel threshold with O.O. refinement there is a significant improvement of the extracted descriptors. In Fig. 7 to Fig. 10 we find as an example the attributes generated in the comparison of the scenes of Cycle 8, expressed in Fig. 5, with bi temporal analysis between the images of 01/15/2019 and 02/02/2019 which represent areas with expressive heterogeneity.

As can be seen in Fig. 7, the application of O.O. refinement and the use of the filter decrease the entropy in clusters extracted by the multilevel threshold. Considering the entropy values for the complete scene, for image 1 (01/15/2019) before O.O. refinement and without applying the filter, the highest entropy value was obtained for class 11, out of the 15 classes initially detected for the scene, with a maximum entropy of 2.48. For image 2 (02/02/2019), the highest value was for class 8, with 16 classes initially detected, with maximum entropy of 3.09.

After refining O.O. by Scale, for image 1 the maximum Entropy value decreased to 2.2 and now for class 2 the maximum of 7 classes detected after refining. For image 2, the maximum entropy value is now 3.0 and for class 4 it is 5 classes detected. With the application of the filter, the values before and after the refinement increase from 3.09 to 2.89 in image 1 and from 3.14 to 3.04 in image 2. Thus, the Entropy descriptor shows that when the multilevel thresholding with OBIA and filter is performed, there is a significant improvement in the impurity within the clusters, thus making the segments more homogeneous and the thresholding classification with better assertiveness tendency.

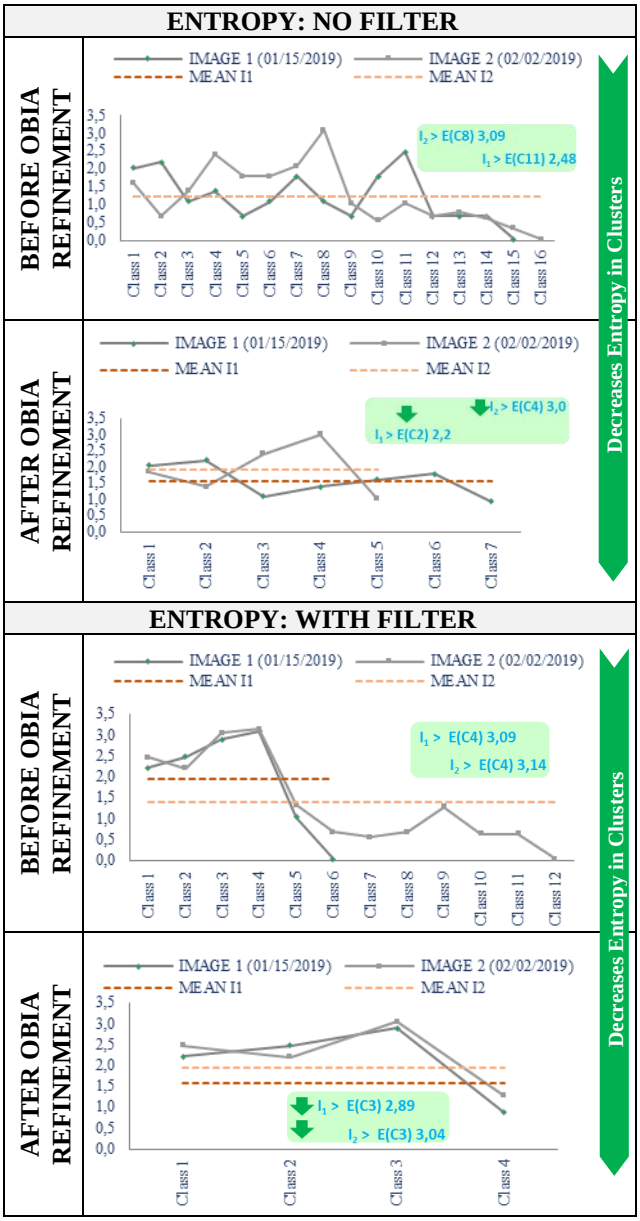

Fig. 7: Entropy: Comparative Before and After OBIA Refining by Scale and Before and After Filter Application.

As can be seen in Fig. 8, the application of O.O. refinement and the use of the filter increase the homogeneity in the clusters extracted by the multilevel thresholding. Considering the homogeneity values for Fig. 1 (01/15/2019) before O.O. refinement and without application of the filter, the extracted homogeneity values of the threshold classes ranged from 0.57 to 0.82. For image 2, the values were in the range 0.62 to 0.89. After the O.O. refinement by scale, for image 1 the homogeneity values were in the range from 0.59 to 0.82 and for image 2 they remained from 0.62 to 0.89. With the application of the filter, the values before and after the refinement went from 0.70 to 0.83 to 0.72 to 0.83 in image 1 and from 0.66 to 0.87 to 0.68 to 0.87 in image 2, increasing in both scenarios the minimum values of homogeneity in the classes. Thus, the descriptor of Homogeneity, which varies from 0 to 1, shows that when the multilevel thresholding with OBIA and filter is performed, there is a significant improvement in homogeneity within the clusters, making the segments more homogeneous and the thresholding classification with better assertiveness tendency.

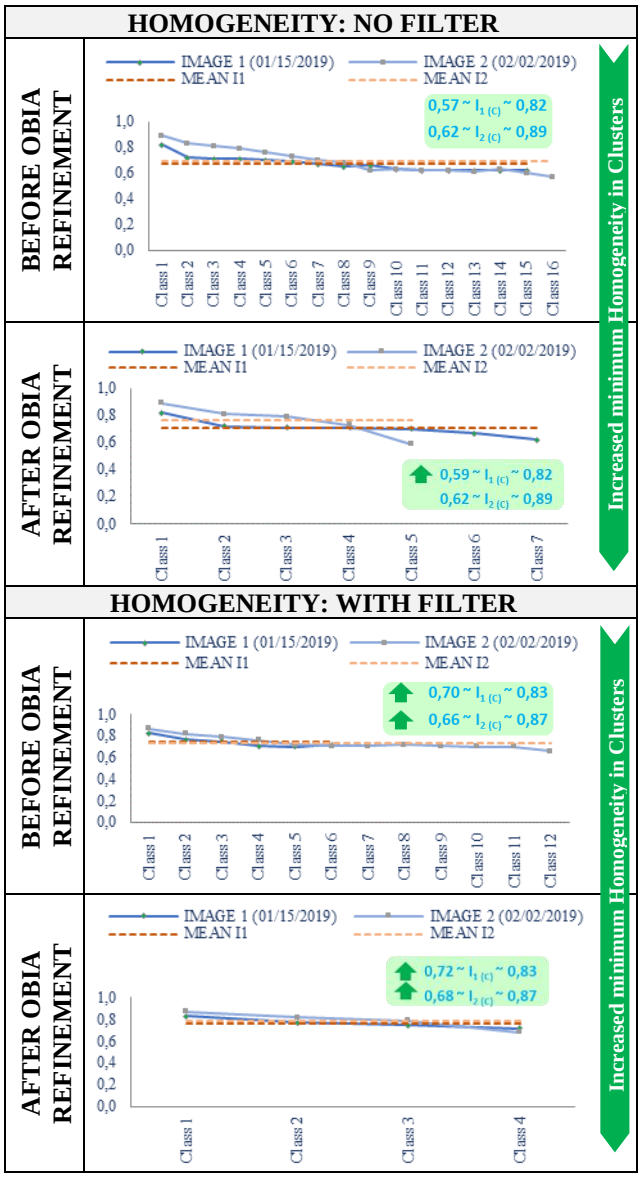

Fig. 8: Homogeneity: Comparative Before and After OBIA Refinement by Scale and Before and After Filter Application.

As can be seen in Fig. 9, the application of O.O. refinement and the use of the filter increase the Correlation in the classes extracted by the multilevel threshold. Considering the correlation values for image 1 (01/15/2019) before O.O. refinement and without the application of the filter, the values extracted from the threshold classes ranged from 0.97 to 0.99, as well as for

image 2. After O.O. refinement by scale, for image 1 the correlation values ranged from 0.98 to 0.99 and for image 2 they remained from 0.97 to 0.99. With the application of the filter, the values before and after refining remained at the nearly maximum descriptor values ranging from 0.99 to 1.0 for both images. Thus, the correlation descriptor, which varies from -1 to 1, demonstrates the similarity between the pixels of the threshold classes, that is, when the multilevel threshold with OBIA and filter is performed, there is significant improvement in the correlation of pixels within the clusters, making the segments more similar and the threshold classification with better assertiveness tendency.

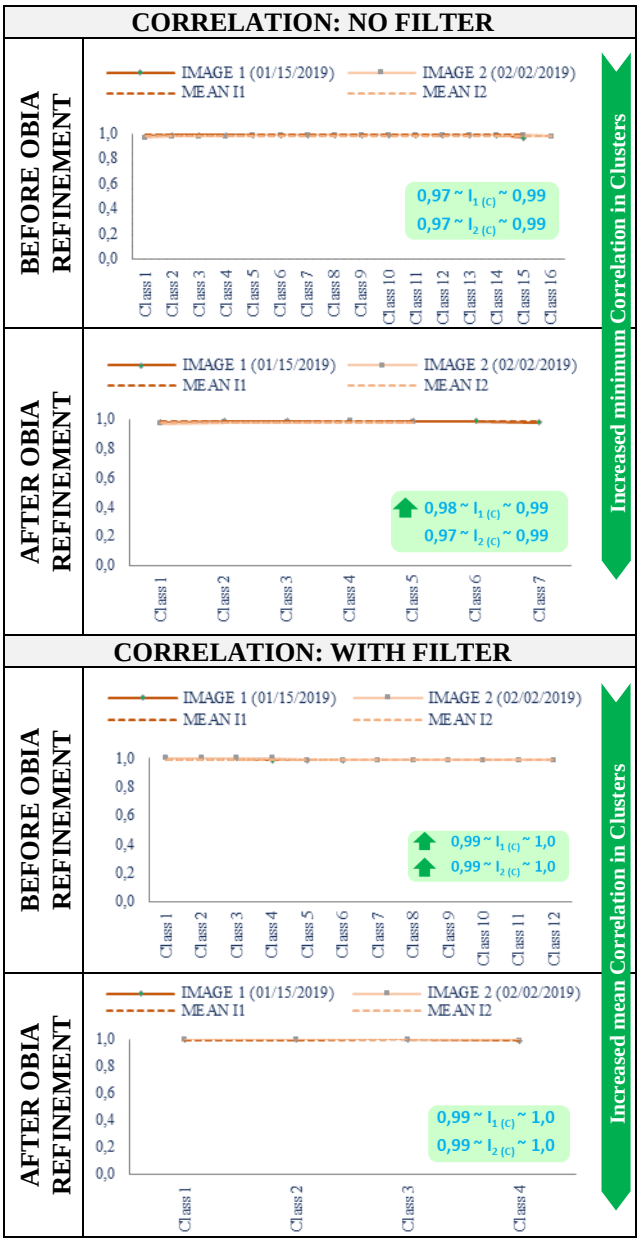

Fig. 9: Correlation: Comparative Before and After OBIA Refining by Scale and Before and After Filter Application.

As can be seen in Fig. 10, the application of O.O. refinement and the use of the filter increase the Euclidean distance between clusters, that is. the separability between the clusters or classes extracted by the multilevel threshold.

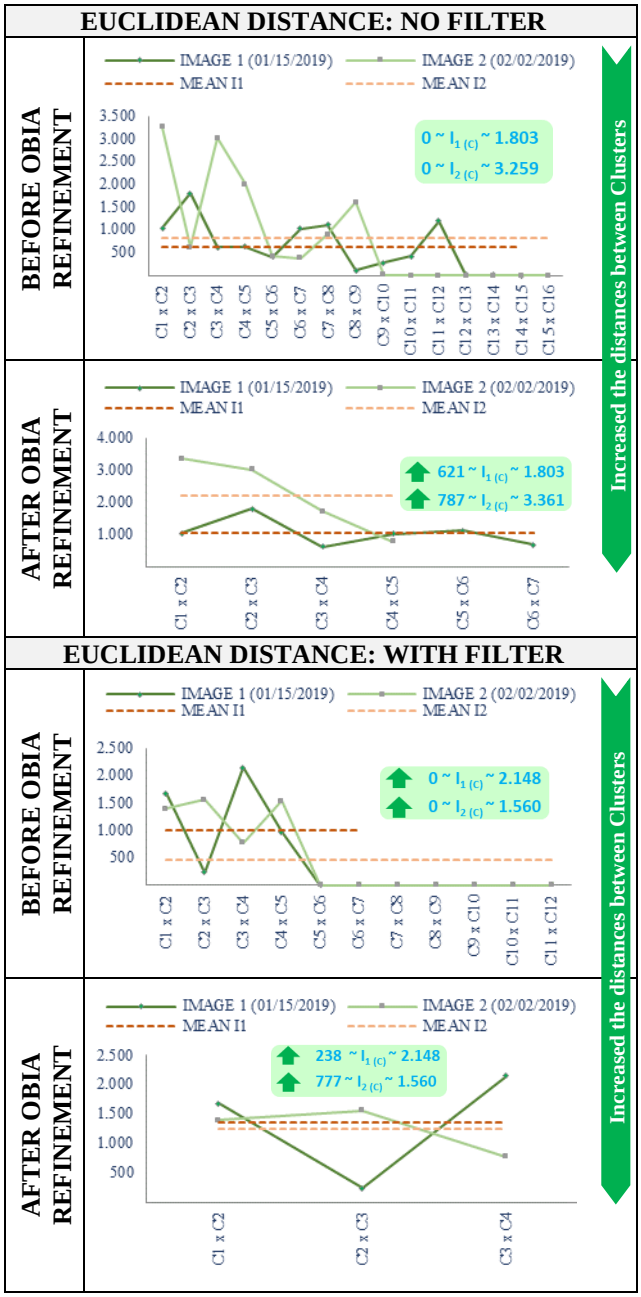

Fig. 10: Euclidean Distance: Comparative Before and After OBIA Refinement by Scale and Before and After Filter Application.

Considering the distance values for image 1 (01/15/2019) before O.O. refinement and without applying the filter, the values extracted from the threshold classes ranged from 0 to 1.803 for image 1 and from 0 to 3.259 for image 2. After O.O. refinement. With the application of

the filter, the values before and after the refinement went from 0 to 2.148 to 238 to 2.148 in image 1. Thus, the Euclidean Distance descriptor shows that when the multilevel thresholding with OBIA and filter is performed, there is a significant improvement in the separability between the clusters, making the segments more homogeneous in the intra-cluster comparison and more dissimilar in the intercluster comparison, that is, increasing the distance between the segments and making the threshold classification with better assertiveness tendency.

Based on the results presented, it is possible to affirm that in addition to the extracted threshold classifications having had assertive signals of the culture development cycle, representing what actually occurred in the plot by the statistical trend analysis, according to Fig. 5, the visual validation of the signals ratifies the quality of the extracted threshold classification, in addition to the extraction of the descriptors finding that the use of OBIA and filter in the multilevel threshold improves the quality of the segments and consequently the threshold classifications.

Table 3 shows the accuracy metrics extracted for each of the classifications in Fig. 6. Thus, the Global Accuracy (G.A.), the Kappa (K), Tau (T) and the Global Disagreement of each of the classifications were generated, being obtained by the sum of the Quantity Discordance (Q.D.) and the Allocation Discordance (A.D.). To test the statistical significance between the Kappa indexes, for each classification intervals with 95% confidence were constructed for the coefficient, where bilateral Z hypothesis tests were performed in order to verify eventual equalities between the classifications at the level of significance of 5%, and comparisons were made between the classifications of the same model and classifications of different models. Thus, the null hypothesis was accepted or rejected from the comparison of the p-value with the significance level adopted, where considering the tabulated Z-value of 1.96 for the significance level of 5%, the results of the Z-Test classifications above 1.96 or below -1.96 were considered statistically different. Therefore, for classifications with Z calculated between -1.96 and 1.96, the hypotheses of equality between the classifications were accepted.

For the 18 classifications performed, about 33.34% of the classification confusion matrices are statistically equal to the 5% significance level, considering the same parameters for the classifications and study regions, before and after the application of the filter with Object-Oriented refinement by the Scale descriptor. Thus, considering the 95% confidence level, the equivalent classifications are those that had global accuracy at 100% with Kappa and Tau indexes of 1.0. Also, such classifications had the p-value of 1.0, being superior to the significance level of 5% with statistically significant acceptance of the null hypothesis of equality for those classifications. For the other classifications, the p-value was lower than 0.002, a value lower than the 5% significance level with rejection of the null hypothesis of equality among the classifications.

Table. 3: Metrics for the PV Model with OBIA refinement, before and after of the filter.

IMAGES	PEAK AND VALLEY MODEL WITH OBIA						Z-Test $H_0: K_1 = K_2$ $H_1: K_1 \neq K_2$	
	NF YF	G.A. (%)	K	T	Q.D. (%)	A.D. (%)	Z Score	95% Conf
1	NF	72.55	0.49	0.45	26.9	0.5	-187.4	≠
	YF	100	1.0	1.0	0	0		
2	NF	100	1.0	1.0	0	0	0	=
	YF	100	1.0	1.0	0	0		
3	NF	100	1.0	1.0	0	0	0	=
	YF	100	1.0	1.0	0	0		
4	NF	100	1.0	1.0	0	0	0	=
	YF	100	1.0	1.0	0	0		
5	NF	75.25	0.50	0.51	1.3	23.4	-151.3	≠
	YF	100	1.0	1.0	0	0		
6	NF	54.40	0.44	0.45	4.3	41.3	10.36	≠
	YF	51.21	0.41	0.42	11.8	37.0		
7	NF	77.51	0.73	0.74	16.1	6.4	-27.7	≠
	YF	84.90	0.80	0.81	11.8	3.3		
8	NF	58.81	0.51	0.52	22.1	19.1	-53.9	≠
	YF	77.13	0.68	0.70	7.7	15.1		
9	NF	84.04	0.80	0.80	4.6	11.4	-50.6	≠
	YF	93.75	0.91	0.92	1.8	4.5		
Mean	**NF**	**80.28**	**0.72**	**0.72**	**8.38**	**11.34**		
	YF	**89.67**	**0.87**	**0.87**	**3.68**	**6.67**		
Median	**NF**	**77.51**	**0.73**	**0.74**	**4.35**	**6.40**		
	YF	**100**	**1.0**	**1.0**	**0**	**0**		

* NF: No Filter; YF: Yes Filter; G.A.: Global Accuracy; K: Kappa Coefficient; T: Tau Index; Q.D.: Quantity Disagreement; A.D.: Allocation Disagreement; 95% Conf: 95% Confidence; ≠: Classifications are Differents; =: Classifications are Equals.

With the results of the classifications, we noticed variations between the different agricultural practices

present in the short and annual cycle plot in terms of accuracy, where more homogeneous areas with less variation in the time of the crop development cycle had greater assertiveness and less errors in the models. Thus, the more heterogeneous the crops within the stand, that is, crop diversity - according to the images in Cycles 6, 7 and 8, there is a tendency to be less global accuracy and agreement rates compared to crops in the stand with homogeneous areas.

Considering the mean and median values presented in Table 3, it is evident that the use of the filter aggregated to the OBIA refinement in the multilevel threshold, presenting higher classification results in relation to the model before the application of the filter. As compared in Table 4 with the mean and median values of the classifications performed for the complete development cycle of the plot, in the analyses performed, when the PV model was applied by multilevel thresholding with OBIA and filter, the results of global accuracy in median was 100%, being 29% higher in comparison with OBIA without application of the filter, with 77.51%.

Table. 4: Comparisons of mean and median values for the PV Model Classifications.

		Model PV^1	Model PV^2	ΔPV^1 x ΔPV^2
Mean	**G.A. (%)**	80.28	**89.67**	11.7%
	Kappa	0.72	**0.87**	20.8%
	Tau	0.72	**0.87**	20.8%
	Q.D. (%)	8.38	**3.68**	-56.0%
	A.D. (%)	11.34	**6.67**	-41.2%
Median	**G.A. (%)**	77.51	**100**	29.0%
	Kappa	0.73	**1.0**	36.9%
	Tau	0.74	**1.0**	35.1%
	Q.D. (%)	4.35	**0**	-
	A.D. (%)	6.40	**0**	-

PV^1: Peaks and Valleys Model Without application of the Filter and with Object-Oriented Refinement by the Scale Descriptor.
PV^2: Peaks and Valleys Model With Filter Application and Object Oriented Refinement by the Scale Descriptor.

The Kappa and Tau agreement rates had a median value of 1.0, being respectively 36.9% and 35,1% higher in comparison with OBIA without application of the filter. While the global median disagreement of quantity and allocation was 0% for the PV model by multilevel thresholding with OBIA and filter, the values were 4.35% and 6.40% respectively in comparison with the multilevel thresholding complemented with OBIA, but without the application of the filter. Considering the values in average, the variation in the measures of accuracy, agreement and disagreement are slightly smaller, however, the results with the application of filter and OBIA are still more expressive.

Fig. 11 shows the 95% confidence intervals (C.I.) for each of the Kappa coefficients obtained for the classifications performed. The C.I. takes into account the standard error, which is obtained by dividing the standard deviation by the square root of the sample size.

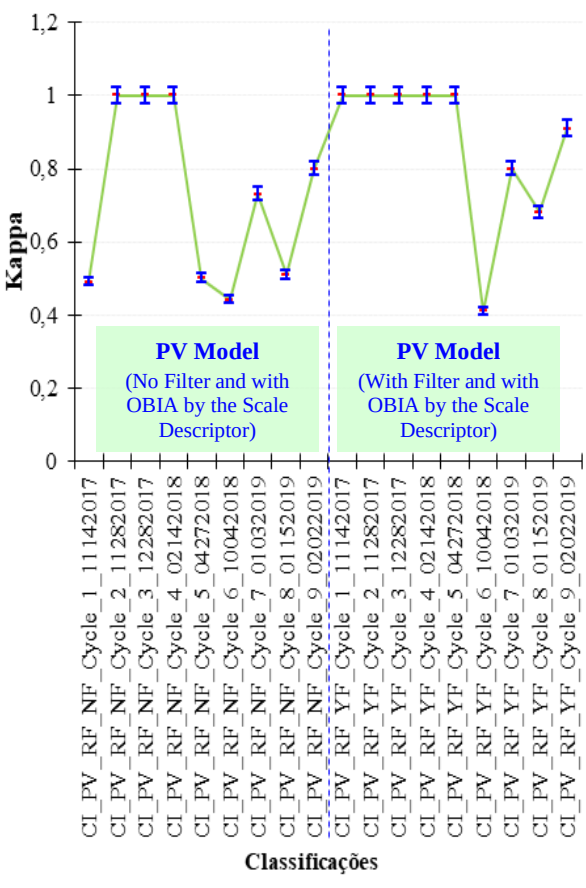

*CI_PV_RF_NF (Classification Confidence Interval for Peaks and Valleys Model with Object-Oriented Refinement by the Scale Descriptor and without Filter);
*CI_PV_RF_YF (Classification Confidence Interval for Peaks and Valleys Model with Object-Oriented Refinement by the Scale Descriptor and with Filter).

Fig. 11: Confidence Interval: Comparative Before and After OBIA Refinement by Scale and Before and After Filter Application.

According to Fig. 5 and Fig. 11, from the classifications extracted in the model developed, for the classifications with maximum Kappa value of 1.0 (Cycles 1 to 5), the confidence interval had in the lower limit the value of 0.98, demonstrating the excellence of the classification at the level of significance adopted. For the model after the application of the filter, the lowest Kappa index was for Cycle 6 in the image of 10/04/2018, with value of 0.41. With the 95% confidence interval, the value range for this classification varied from 0.40 to 0.42. From the visual inspection of the scene, although initially it seems to present low diversity in the plot and there are characteristics of exposed soil, different nuances can be observed in the plot, being ratified by the information of 6 classes detected by the threshold originally extracted, according to Fig. 6. Thus, it is likely that the accuracy extracted was impacted by mixtures within the plot, such as soil being prepared for planting, which made it not so homogeneous in the transition period between scenes.

V. CONCLUSION

The application of tool developed in Python, called LimiariZC, with the development of module for Peaks and Valleys model, with Object-Oriented refinement and the use of the filter, presented significant results of classifications, where it was found that in the multilevel threshold present in the PV model, when OBIA information is incorporated in addition to the use of filters, of medium convolution passes low, the results are more assertive. The different methods present in the literature regarding thresholding, aiming to find optimal thresholds of separability by different techniques [2] [32] [62] [81], in a macro way present high computational cost, complexity, high specificity and low robustness, and in general do not aggregate the contextual information allowing the O.O. refinement of the classes, which according to the results presented in the proposed approach showed to have the best accuracy.

Moreover, the low response time in processing - around 25 seconds for execution of the model for areas of up to 100 ha, which represent almost 90% of the rural properties in the country, contemplating in processing the emission of signals - with reduced investment cost, add innovation and differential technology, making the proposed method effective and attractive.

The decision tree built for the emission of automated signals for the detection of changes in the multilevel thresholding model, by means of an analysis of statistical trend from the extraction of a set of variables and descriptors that demonstrated a standard behavior of knowledge for remote monitoring of crops, proved to be significant in the emission of warning signals of loss of vegetation or warning of vegetative growth. The tree originated from the proposed method aimed that the attributes would direct the hierarchical tree, without the substitution of the parameters by the repetitivity employed in traditional decision tree algorithms such as J48, Random Tree, Random Forest, REPTree, Logistical Model Trees among others [27] [29] [37] [45] [49] [83], in order to find the best separability attribute.

The results indicated that the attributes extracted from Entropy, Homogeneity, Correlation, Euclidean Distance and Coefficient of Variation, whether extracted intra-clusters or inter-clusters, were positively affected with the use of the multi-level threshold with OBIA aggregated to the use of the filter. Although the work demonstrates the effectiveness of the descriptors to ratify the improvement of the clusters extracted by the automated multi-level thresholding with O.O. refinement and application of the filter, the use of descriptors in the monitoring corroborates with studies presented in which they proved feasible for the detection of changes [44] [46]. In the comparison of images with filter before and after O.O. refinement, it was observed that when the image goes through a filtering process, with smoothing of the short peaks and shallow valleys in the histograms, the filter decreases the Total Coefficient of Variation of the scene indicating less dispersion around the mean and improvement of the accuracy in the threshold classification. Also, the descriptors extracted indicated an improvement in the degree of impurity within the classes, making the groupings more similar, with greater homogeneity of pixels and classes more uniform, and correlation between pixels with improved threshold classification. Thus, it was detected that the separability between classes increased, demonstrating greater group isolation and a more precise classification with more dissimilar clusters when compared to each other.

Thus, with the set of results, it was possible to assess the quality of the proposed method and its feasibility for remote monitoring in agricultural productions, where the alert/warning emissions showed assertive results in all tests demonstrating the feasibility of attending in the mitigation of risks in the fundable area, without necessarily having on-site visits.

The results obtained showed that the model can be used as a significant indicator of oscillation and multitemporal trends in land use and cover for detecting changes without necessarily carrying out on-site visits and in line with the Government Consultancy for agricultural financings with the recommendation of the Central Bank of Brazil and which can be extended to other countries due to population growth and the need for new areas for planting with the

consequent release of agricultural credits. Thus, the methodology aims to monitor the development of cultures, reducing face-to-face work. Finally, although the models were applied in a study area in Brazil, can be used in any region of the planet for monitoring areas with agricultural financings or that will be financed, allowing greater control and inspection by those responsible for releasing agricultural credit, that usually has government subsidies.

REFERENCES

[1] Aboud Neta, S. R.; Bias, E. S. (2021). "Remote Sensing for Risk Mitigation in Agricultural Financings: Multitemporal Change Detections in Agricultural Areas using the Delta NIR and Delta NDVI Models". International Journal of Advanced Engineering Research and Science, 8 (8): 276-297. doi: 10.22161/ijaers.88.32.

[2] Akay, B. (2013). "A study on particle swarm optimization and artificial bee colony algorithms for multilevel thresholding". Applied Soft Computing, 13 (6): 3066-3091. doi: 10.1016/j.asoc.2012.03.072.

[3] Albuquerque, M. P.; Esquef, I. A.; Mello, A. G. (2004) "Image thresholding using Tsallis entropy". Pattern Recognition Letters, 25 (9): 1059-1065. doi: 10.1016/j.patrec.2004.03.003.

[4] Alexandratos, N., Bruinsma, J. (2012). "World agriculture towards 2030/2050: the 2012 revision". doi: 10.22004/ag.econ.288998.

[5] Azeredo, M., Monteiro, A. M. V., Escada, M. I. S., Ferreira, K. R., Vinhas, L., Pinheiro, T. F. (2016). "Mineração de trajetórias de mudança de cobertura da terra em estudos de degradação florestal". Revista Brasileira de Cartografia, 68 (4): 717-731.

[6] Baatz, M.; Schape, A. (2000). "Multiresolution segmentation: an optimization approach for high quality multi-scale image segmentation". In: XII Angewandte Geographische Informations verarbeitung, AGIT Symposium. Proceedings. Karlsruhe, Alemanha: Herbert Wichmann Verlag, Salzburg - Áustria, 12-23.

[7] BACEN. (2015). Banco Central do Brasil. Resolução nº 4.427, de 25 de Junho de 2015. 2015. Diário Oficial da República Federativa do Brasil.

[8] Baraldi, A.; Boschetti, L. (2012). "Operational Automatic Remote Sensing Image Understanding Systems: Beyond Geographic Object-Based and Object-Oriented Image Analysis (GEOBIA/GEOOIA). Part 1: Introduction". Remote Sensing, 4 (12): 2694-2735. doi: 10.3390/rs4092694.

[9] Barbieri, A. L.; De Arruda, G. F.; Rodrigues, F. A.; Bruno, O. M.; Da Fontoura Costa, L. (2011). "An entropy-based approach to automatic image segmentation of satellite images". Physica A: Statistical Mechanics and its Applications, 390 (3): 512-518. doi: 10.1016/j.physa.2010.10.015.

[10] Bardossy, A; Samaniego, L. (2002). "Fuzzy rule-based classification of remotely sensed imagery". IEEE Transactions on Geosciences and Remote Sensing, 40 (2). Doi: 10.1109/36.992798.

[11] Bhargavi, K.; Jyothi, S. (2014). "A survey on threshold based segmentation technique in image processing". International Journal of Innovative Research and Development, 3 (12): 234-239.

[12] Blaschke, T. (2010). "Object based image analysis for remote sensing". ISPRS Journal of Photogrammetry and Remote Sensing, 65 (1): 2-16. doi: 10.1016/j.isprsjprs.2009.06.004.

[13] Bonato, M. (2009). "Projeto Agrobrasília". Universidade de Brasília, Brasília. doi: 10.26512/2008.08.TCC.339.

[14] Campbell, J. B.; Wynne, R. H. (2011). "Introduction to Remote Sensing". New York: The Guilford Press, 683p.

[15] Castanheira, P. (2005). "Estatística aplicada a todos níveis". Curitiba: Editora Ibpex. 2ª ed. 310 p.

[16] Chen, X.; Chen, J.; Shi, Y.; Yamaguchi, Y. (2012). "An automated approach for updating land cover maps based on integrated change detection and classification methods." ISPRS Journal of Photogrammetry and Remote Sensing, 71: 86-95. doi: 10.1016/j.isprsjprs.2012.05.006.

[17] CNA. (2020). "Confederação da Agricultura e Pecuária do Brasil". PIB do Agronegócio. Brasília.

[18] Crosta, A. P. (2002). "Processamento Digital de Imagens de Sensoriamento Remoto". Campinas: Instituto de Geociências - UNICAMP.

[19] Davies, D. L.; Bouldin, D. W. (1979). "A cluster separation measure". IEEE transactions on pattern analysis and machine intelligence (2): 224-227. doi: 10.1109/TPAMI.1979.4766909.

[20] Ehlers, M.; Sofina, N.; Filippovska, Y.; Kada, M. (2014). "Automated techniques for change detection using combined edge segment texture analysis, GIS, and 3D information". In: Global urban monitoring and assessment through Earth observation. CRC Press, 346-373. doi: 10.1201/B17012-22.

[21] EMBRAPA, Empresa Brasileira de Pesquisa Agropecuária. (2021). Estudos socioeconômicos e ambientais. "O Agro no Brasil e no Mundo: Uma Síntese do Período de 2000 a 2020".

[22] FAOSTAT, Food and Agriculture Organization of the United Nations. (2018). "Major Commodities Exporters. Countries by Commodity". Rankings.

[23] Flemming, D. M.; Gonçalves, M. B. (1992). "Cálculo A – Funções, Limite, Derivação, Integração". Makron Books. 5ª Ed. São Paulo.

[24] Florenzano, T. G. (2011). "Iniciação em Sensoriamento Remoto. 3ª ed.", S.P: Oficina de Texto.

[25] Frizzarini, C.; Lauretto, M. S. (2013). "Proposta de um Algoritmo para indução de árvores de classificação para dados desbalanceados". Escola de Artes, Ciências e Humanidades – Universidade de São Paulo (USP). São Paulo.

[26] Ghesti, L. V. (2009). "Programa de assentamento dirigido do Distrito Federal – PAD/DF: Uma realidade que superou o sonho". Brasília.

[27] Giasson, E.; Hartemink, A. E.; Tornquist, C. G.; Teske, R.; Bagatini, T. (2013). "Avaliação de cinco algoritmos de

árvores de decisão e três tipos de modelos digitais de elevação para mapeamento digital de solos a nível semidetalhado na Bacia do Lageado Grande, RS, Brasil". Ciência Rural, 43 (11): 1967-1973. doi: 10.1590/S0103-84782013001100008.

[28] Graça, M. L. A. (2004). "Monitoramento e Caracterização de Áreas Submetidas à Exploração Florestal na Amazônia por Técnicas de Detecção de Mudanças", 275 p. INPE-13644-TDI/1046). Tese (Doutorado em Sensoriamento Remoto) - Instituto Nacional de Pesquisas Espaciais, São José dos Campos.

[29] Hall, M.; Frank, E.; Holmes, G.; Pfahringer, B.; Reutemann, P.; Witten, I. H. (2009). "The WEKA Data Mining Software: an update". ACM SIGKDD explorations newsletter, 11(1): 10-18. doi: 10.1145/1656274.1656278.

[30] Haralick, R. M.; Shanmugam, K.; Dinstein, I. H. (1973). "Textural features for image classification. IEEE Transactions on systems, man, and cybernetics". (6): 610-621. doi: 10.1109/TSMC.1973.4309314.

[31] Hay, G. J.; Castilla, G. (2008). "Geographic Object-Based Image Analysis (GEOBIA): A new name for a new discipline". In: Object-based image analysis. Springer Berlin Heidelberg, 75-89. doi: 10.1007/978-3-540-77058-9_4.

[32] Horgn, M. (2011). "Multilevel thresholding selection based on the artificial bee colony algorithm for image segmentation". Expert Systems with Applications, 38 (11): 13785-13791. doi: 10.1016/j.eswa.2011.04.180.

[33] Hou, Z.; Hu, Q.; Nowinski, W. L. (2006). "On minimum variance thresholding". Pattern Recognition Letters, 27 (14): 1732-1743. doi: 10.1016/j.patrec.2006.04.012.

[34] Hussain, M.; Chen, D.; Cheng, A.; Wei, H.; Stanley, D. (2013). "Change detection from remotely sensed images: From pixel-based to object-based approaches". ISPRS Journal of Photogrammetry and Remote Sensing, 80: 91-106. doi: 10.1016/j.isprsjprs.2013.03.006.

[35] IBGE. Instituto Brasileiro de Geografia e Estatística. Censo Agropecuário. (2017). ISSN 0103-6157. Rio de Janeiro, Ministério do Planejamento, Desenvolvimento e Gestão, 7: 1-108.

[36] Ilkin, S.; Hangişi, F. S.; Şahin, S. (2017). "Comparison of global histogram-based thresholding methods that applied on wound images". International Journal of Computer Applications, 975: 8887. doi: 10.5120/ijca2017914002.

[37] Immitzer, M; Atzberger, C; Koukal, T. (2012). "Tree species classification with random forest using very high spatial resolution 8-band WorldView-2 satellite data". Remote Sensing, 4 (9): 2661-2693. doi: 10.3390/rs4092661.

[38] Incra. Instituto Nacional de Colonização e Reforma Agrária. (2018). "Estatísticas Cadastrais. Estrutura Fundiária Brasil". Brasília, Ministério da Agricultura.

[39] Jensen, J. R. (2009). "Sensoriamento Remoto do ambiente: Uma perspectiva em recursos terrestres". São José dos Campos: Parêntese, 604 p.

[40] Kalmegh, S. (2015). "Analysis of weka data mining algorithm reptree, simple cart and randomtree for classification of indian news". International Journal of Innovative Science, Engineering & Technology, 2 (2): 438-446.

[41] Kandwal, R.; Kumar, A.; Bhargava, S. (2014). "Existing image segmentation techniques". International Journal of Advanced Research in Computer Science and Software Engineering, 4 (4): 153-156.

[42] Kapur, J. N.; Sahoo, K.; Wong, K. C. (1985). "A new method for gray-level Picture thresholding using the entropy of the histogram". Computer Vision, Graphics and Image Processing, 29: 273-285. doi: 10.1016/0734-189X(85)90125-2.

[43] Khanna, N., Solanki, N. (2014). "Role of agriculture in the global economy". 2nd International Conference on Agricultural & Horticultural Sciences. Hyderabad, India. Agrotechnol. 2:4. doi:10.4172/2168-9881.S1.008.

[44] Khurana, M; Saxena, A. (2017). "Exploring the effectiveness of various texture features for change detection in remote sensing images". In: 2017 International Conference on Computer, Communications and Electronics (Comptelix). IEEE, 96-100. doi: 10.1109/COMPTELIX.2017.8003945.

[45] Landwehr, N.; Hall, M.; Frank, E. (2005). "Logistic model trees. Machine learning", 59 (1-2): 161-205.

[46] Li, M.; Ma, L.; Blaschke, T.; Cheng, L.; Tiede, D. (2016). "A systematic comparison of different object-based classification techniques using high spatial resolution imagery in agricultural environments". International Journal of Applied Earth Observation and Geoinformation, 49: 87-98. doi: 10.1016/j.jag.2016.01.011.

[47] Liao, S.; Chen, T. S.; Chung, C. (2001). "A fast algorithm for multilevel thresholding". J. Inf. Sci. Eng., 17 (5): 713-727.

[48] Liu, W. T. H. (2015). "Aplicações de Sensoriamento Remoto". Oficina de Textos.

[49] Lorenzett, C. D. C.; Telocken, A. V. (2016). "Estudo Comparativo entre os algoritmos de Mineração de Dados Random Forest e J48 na tomada de Decisão". Simpósio de Pesquisa e Desenvolvimento em Computação, 2 (1).

[50] Malyszko, D.; Stepaniuk, J. (2010). "Adaptive multilevel rough entropy evolutionary thresholding". Information Sciences, 180 (7): 1138-1158. doi: 10.1016/j.ins.2009.11.034.

[51] Martinelli, L. A., Joly, C. A., Nobre, C. A., Sparovek, G. (2010). "A falsa dicotomia entre a preservação da vegetação natural e a produção agropecuária". Biota Neotropica, 10 (4): 323-330. doi: 10.1590/S1676-06032010000400036.

[52] Meneses, R.; Almeida, T. (2012). "Introdução ao processamento de imagens de Sensoriamento Remoto". Universidade de Brasília, Brasília.

[53] Narkhede, H. P. (2013). "Review of image segmentation techniques". International Journal of Science and Modern Engineering, 1 (8): 54-61.

[54] Navulur, K. (2006). "Multispectral image analysis using the Object-Oriented paradigm". Taylor & Francis Group, Boca Raton, USA. 165 p. doi: 10.1201/9781420043075.

[55] Neves, A. A.; Silva, E. J.; Roter, J. M.; Belladona, F. G.; Alves, H. D.; Lopes, R. T.; Paciornik, S.; De-Deus, G. A. (2015). "Exploiting the potential of free software to evaluate root canal biomechanical preparation outcomes through

micro-CT images". International endodontic journal, 48 (11): 1033-1042. doi: 10.1111/iej.12399.

[56] Novack, T; Kux, H. J. (2010). "Urban land cover and land use classifi cation of an informal settlement area using the open-source knowledge-based system InterIMAGE". Journal of Spatial Science, 55 (1): 33-41. doi: 10.1080/14498596.2010.487640.

[57] OECD-FAO. (2020). "Organization for Economic Co-operation and Development and the Food and Agriculture Organization. Agricultural Outlook 2020-2029". Paris: OECD Publishing, doi: 10.1787/19991142.

[58] Oliva, D.; Cuevas, E.; Pajares, G.; Zaldivar, D.; Perez-Cisneros, M. (2013). "Multilevel thresholding segmentation based on harmony search optimization". Journal of Applied Mathematics. doi: 10.1155/2013/575414.

[59] ONU, United Nations. (2015). World Water Development Report2015: Water for a Sustainable World. WWAP (United Nations World Water Assessment Programme). The United Nations, Paris, UNESCO.

[60] Onyiriuba, L., Okoro, E. O., Ibe, G. I. (2020). "Strategic government policies on agricultural financing in African emerging markets". Agricultural Finance Review, 80 (4): 563-588. doi: 10.1108/AFR-01-2020-0013.

[61] Otsu, A. (1978). "A threshold selection method from gray-level histogram". IEEE Transactions on Systems, Man, and Cybernetics, 62-66. doi: 10.1109/TSMC.1979.4310076.

[62] Pare, S.; Bhandari, A. K.; Kumar, A.; Singh, G. K.; Khare, S. (2015). "Satellite image segmentation based on different objective functions using genetic algorithm: a comparative study". In: IEEE international conference on digital signal processing (DSP). IEEE, 730-734. doi: 10.1109/ICDSP.2015.7251972.

[63] Peiman, R. (2011). "Pre-classification and post-classification change-detection techniques to monitor land-cover and land-use change using multi-temporal Landsat imagery: a case study on Pisa Province in Italy". International Journal of Remote Sensing, 32 (15): 4365-4381. doi: 10.1080/01431161.2010.486806.

[64] Pessoa, S. P., Galvanin, E. A. D., Kreitlow, J. P., Neves, S. M., Nunes, J. R., Zago, B. W. (2013). "Análise espaço-temporal da cobertura vegetal e uso da terra na Interbacia do Rio Paraguai Médio-MT, Brasil". Revista Árvore, 37 (1): 119-128. doi: 10.1590/S0100-67622013000100013.

[65] Planetlabs. (2016). "Planet Imagery Product Specification: PlanetScope & Rapideye".

[66] Ribeiro, M. C.; Metzger, J. P.; Martensen, A. C.; Ponzoni, F. J.; Hirota, M. M. (2009). "The Brazilian Atlantic Forest: how much is left, and how is the remaining forest distributed? Implications for conservation". Biological Conservation, 142 (6): 1141-1153. doi: 10.1016/j.biocon.2009.02.021.

[67] Sahoo, K.; Arora, G. (2004). "A thresholding method based on two-dimensional Renyi's entropy". Pattern Recognition, 37 (6): 1149-1161. doi: 10.1016/j.patcog.2003.10.008.

[68] Sarkar, S.; Das, S.; Chaudhuri, S. (2015). "A multilevel color image thresholding scheme based on minimum cross entropy and differential evolution". Pattern Recognition Letters, 54: 27-35. doi: 10.1016/j.patrec.2014.11.009.

[69] Scolari, D. (2009). "Produção agrícola mundial: o potencial do Brasil".

[70] Senger, L.; Gouveia, L. (2010). "Aplicação de redes neurais ART e análise de textura para classificação do estado de alteração de agregados minerais". Revista de Informática Teórica e Aplicada, 17 (1): 31-51. doi: 10.22456/2175-2745.9644.

[71] Sezgin, M.; Sankur, B. (2004). "Survey over image thresholding techniques and quantitative performance evaluation". Journal of Electronic Imaging, 13 (1): 146-166. doi: 10.1117/1.1631315.

[72] Shannon, C. E. (1948). "A Mathematical Theory of Communication". The Bell System Technical Journal, 27 (3): 379-42. doi: 10.1002/j.1538-7305.1948.tb01338.x.

[73] Svetlana, P., Irena, J., Zaklina, S. (2018). The importance of bank credits for agricultural financing in Serbia. 65 (1). doi: 10.5937/ekoPolj1801065P.

[74] Tewkesbury, A. P.; Comber, A. J.; Tate, J.; Lamb, A.; Fisher, F. (2015). "A Critical Synthesis of Remotely Sensed Optical Image Change Detection Techniques". Remote Sensing of Environment, 160 (1): 1-14. doi: 10.1016/j.rse.2015.01.006.

[75] Tokas, N.; Karkra, S.; Pandey, M. K. (2016). "Comparison of Digital image segmentation techniques-a research review". International Journal of Computer Science and Mobile Computing, 5 (5): 215-220.

[76] Torres-Vera, M. A.; Prol-Ledesma, R. M.; Garcia-Lopez, D. (2009). "Three decades of land use variations in Mexico City". International Journal of Remote Sensing, 30 (1): 117-138. doi: 10.1080/01431160802261163.

[77] Wang, Q.; Chen, J.; Tian, Y. (2008). "Remote sensing image interpretation study serving urban planning based on GIS". In: XXXVII International Archives of the Photogrammetry, Remote Sensing and Spatial Information Sciences. Proceedings. Beijing, China, 453-456.

[78] Weckmüller, R.; Vicens, R. S. (2016). "Método híbrido de detecção de mudanças: uma associação entre classificação baseada em objetos e baseada em pixels". Revista Brasileira de Cartografia, 68 (5): 883-899.

[79] Yan, F.; Zhang, H.; Kube, C. R. (2005). "A multistage adaptive thresholding method". Pattern recognition letters, 26 (8): 1183-1191. doi: 10.1016/j.patrec.2004.11.003.

[80] Yin, Y. (2007). "Multilevel minimum cross entropy threshold selection based on particle swarm optimization". Applied mathematics and computation, 184 (2): 503-513. doi: 10.1016/j.amc.2006.06.057.

[81] Yuan, X.; Wu, L.; Peng, Q. (2015). "An improved Otsu method using the weighted object variance for defect detection". Applied Surface Science, 349: 472-484. doi: 10.1016/j.apsusc.2015.05.033.

[82] Zhang, H. (2009). "Comparison of Investment and Financing Systems in Foreign Agriculture and Their Enlightenments for China". Asian Social Science. doi: 10.5539/ass.v5n12p60.

[83] Zhu, Z.; Woodcock, C. E. (2014). "Continuous change detection and classification of land cover using all available Landsat data". Remote Sensing of Environment, 144: 152-171. doi: 10.1016/j.rse.2014.01.011.